Available online at www.sciencedirect.com
ScienceDirect
Ceramics International 36 (2010) 1561–1569
CERAMICS INTERNATIONAL
www.elsevier.com/locate/ceramint

Compressive strength and preliminary *in vitro* evaluation of gypsum and gypsum–polymer composites in protein-free SBF at 37 °C

H.F. El-Maghraby [a,1], O. Gedeon [a], D. Rohanova [a], Y.E. Greish [b,*]

[a] *Institute of Chemical Technology, ICT, Department of Glass and Ceramics, Technicka 5, Praha 6, 166 28, Czech Republic*
[b] *Department of Chemistry, UAE University, Maqam Campus, Al Ain, P.O. Box 17551, United Arab Emirates*

Received 12 October 2009; received in revised form 3 January 2010; accepted 5 February 2010
Available online 9 March 2010

Abstract

Gypsum is a bioresorbable material that has been used in many applications such as tissue regeneration. Mechanical properties of gypsum have limited its applications to non-load bearing sites. The current study aimed at studying the compressive strength and behaviour of gypsum–polymer composites in protein-free simulated body fluids (SBF). Polymers studied were poly(vinyl alcohol) (PVA) and its copolymers with vinyl acetate and itaconic acid in addition to vinyl acetate and vinyl chloride. Composites with the highest compressive strength results were chosen for the preliminary *in vitro* evaluation in protein-free SBF solutions. Changes in the concentrations of Ca^{2+} and PO_4^{3-} ions, weight loss and morphology of the solid samples were monitored after soaking them in SBF and 1.5 SBF solutions. Results showed resorption of gypsum, concurrently with deposition of apatite in all composites, including polymer-free gypsum. Mechanical integrities of all samples were maintained, suggesting their stabilities when used as bone cements.

Keywords: Gypsum; Hydroxyapatite; Biomimetic; Microstructure; Compressive strength

1. Introduction

Gypsum is considered a highly biocompatible material that is one of the simplest synthetic bone graft materials with the longest clinical history, spanning more than 100 years [1]. It is classified as a bioresorbable material, whose resorption products integrate with the different cycles in the human body. It has been successfully used to treat periodontal disease, endodontic lesions, alveolar bone loss, and maxillary sinus augmentation [1]. It has been used as a binder to facilitate healing and prevent loss of grafting materials, which is also attributed to its tissue compatibility [2]. Gypsum-containing biomaterials have also exhibited promise as grafts in a preclinical repair model of interabony periodontal defects, as well as in clinical reports for sinus augmentation and treatments of femoral shaft nonunions [3,4]. Plaster of Paris, which is considered a gypsum precursor, was previously shown to improve the setting reactions of a biodegradable calcium phosphate cement [5]. Due to their chemical composition and porous structure, these gypsum-containing cements combined both the resorbability and osteoconductivity [6]. Sato et al. further indicated the promising characteristics of gypsum after mixing it with apatite particles, based on the relatively fast absorption of gypsum without interfering with the process of bone healing [7]. In an attempt to use gypsum as a bone graft substitute for lumbar spinal fusion, however, gypsum showed unsuccessful results because of its rapid resorption [8]. Plaster of Paris was also added to a calcium phosphate cement, producing a biodegradable bone cement that was used for bone reconstruction [9]. The advantage of bioresorption of gypsum was utilized in a composite involving plaster of Paris and a nanocrystalline hydroxyapatite, that was successfully used for the delivery of antibiotics in bone infections [10].

Despite the advantage of bioresorption of gypsum that makes it an attractive candidate for certain applications, its relatively low mechanical properties have limited its scope of application as a bone replacement implant or even as a bone

* Corresponding author. Permanent address: Department of Ceramics, National Research Centre, Cairo, Egypt. Tel.: +971 50 2338203; fax: +971 3 7671291.
E-mail address: y.afifi@uaeu.ac.ae (Y.E. Greish).
[1] Permanent address: Department of Ceramics, National Research Centre, Cairo, Egypt.

0272-8842/$36.00
doi:10.1016/j.ceramint.2010.02.023

cement. Different classes of materials were mixed with gypsum in order to improve its mechanical properties. Blending gypsum with polymers has been considered one of the successful approaches to modulate the mechanical properties of gypsum [11–13]. The presence of certain functional groups on these polymers, such as hydroxyl and carboxyl groups, is mostly favoured. These were found to bind with the calcium sites along the set gypsum products. Polymers that do not have these groups are usually passive throughout the setting reaction of gypsum. However, the mechanical interlocking of these polymers with the set gypsum crystals improves the overall mechanical performance of the produced composites. For biomedical applications, polymers used with gypsum should be biocompatible to avoid rejection by the human immune system. Different polymers could be used in this regard, ranging from bioactive to bioinert, depending on the type and site of application. The current study investigated the formation of gypsum composites with poly(vinyl alcohol) (PVA) and its copolymers with different vinyl moieties. The bioactivity of PVA and its different copolymers was previously investigated and was attributed to the presence of certain functional groups along the neat polymer as well as its copolymers [14–17]. Both hydroxyl (–OH) and carboxylic (–COOH) groups were showed to help in the mineralization of polymers containing these groups, a process that is similar to the mineralization of collagen in nature [18]. Studies on the mineralization of polymers bearing these groups were carried out in solutions containing ions with type and concentrations similar to those existing in the human body, called simulated body fluids; SBF. The ability to induce formation of apatite coatings on composites containing these polymers indicates the strong potential of these composites to bind with natural bone if used as an implant or cement [19]. Although a conclusion of the suitability of a new biomaterial cannot be solely based on using these protein-free SBF solutions, it is still considered a valid approach to preliminary evaluate new biomaterials [19]. This has to be followed by detailed *in vitro* and *in vivo* studies. [20]. The bioactivity of the starting materials used in the current study has been previously established, both *in vitro* and *in vivo*. Gypsum was found to grow an apatite layer on its surface in SBF as well as *in vivo* [21]. In a recent study, PVA substrates coated with apatite showed enhanced an enhanced fibroblast cells adhesion and proliferation compared to uncoated PVA substrates [22]. The current study, therefore, investigates the performance of their combinations in SBF solutions. Composites containing optimum concentrations of the three investigated polymers were subjected to the SBF evaluation experiments. Selection of these optimum composites was made based on the mechanical properties of composites containing different proportions of each of the three polymers. Changes in the solution chemistry of these solutions as a result of the immersion of gypsum and its composites in SBF for up to 2 weeks were followed concurrently with the investigation of changes in the weights of the studied samples. Moreover, morphologies and phase composition of the immersed samples after different periods in the SBF solutions were monitored.

2. Materials and methods

Starting materials used in the current study included plaster of Paris ($CaSO_4 \cdot 1/2H_2O$) (BPB Formula Gmbh, Germany), poly(vinyl alcohol) (Aldrich); PI, poly(vinyl alcohol-*co*-vinyl acetate-*co*-itaconic acid) (Aldrich); PII, and poly(vinyl chloride-*co*-vinyl acetate-*co*-vinyl alcohol) (Aldrich); PIII. Analysis of the plaster starting material revealed a purity of 96% [23]. Composites were made by blending a powder mixture of the plaster of Paris and the solid powder with water. Powder-to-liquid ratio was decided based on a previously determined normal consistency of 46% of neat plaster [23]. Based on preliminary experiments, the following powder mixtures containing plaster of Paris and all polymers were investigated for their mechanical properties:

(a) Plaster of Paris + PI at percentages of 0.25, 0.5, 1.0, 2.0, 3.0, and 4.0 by weight.
(b) Plaster of Paris + PII at percentages of 0.2, 0.4, 0.6, 0.8, 1.0, 1.2, 1.4, 1.6, and 2.0 by weight.
(c) Plaster of Paris + PIII at percentages of 1, 2, 3, 4, 6, and 8 by weight.

Compressive strength measurements were carried out on cubic samples of both neat gypsum and gypsum–polymer composites with dimensions 2.5 cm × 2.5 cm × 2.5 cm. Samples cured at ambient conditions for 7 days were investigated for their compressive strength using a universal testing machine (FPZ100/1, HECKERT/THURINGER INDÜSTRIEWERKE, Germany) at a crosshead speed of 0.56×10^{-4} m/s. The mean value of five measurements for each sample was recorded. Composites with optimum compressive strengths were chosen for the SBF evaluation studies.

For the preliminary *in vitro* evaluation, two types of protein-free simulated body fluids (SBF and 1.5 SBF) were prepared as was previously described [24]. The composition of these solutions is given in Table 1. Two types of treatments were carried out for both neat gypsum and gypsum–polymer composites. In the first set of experiments, pre-weighed rectangular samples with dimensions 2.0 cm × 2.0 cm × 2.0 cm were immersed in 100 cm^3 SBF solution and kept at 37 °C for 2 weeks. Aliquot of 1.5 cm^3 was collected from each solution every day to be analyzed for Ca^{2+}, and PO_4^{3-} ions. Measurements of these ions were carried out in triplicates ($n = 3$), and the average was recorded. In the second set of experiments, the pre-weighed samples were soaked in SBF solution for a week, followed by soaking in 1.5 SBF for another week. At the end of each of the treatments, solid samples were collected, flushed with acetone, completely dried then weighed to determine weight change, if any, and to investigate its morphology changes as a result of immersion in SBF. Microstructural features of Au–Pd alloy-coated samples were investigated by scanning electron microscopy (SEM) (Hitachi, S-4700) equipped with an energy-dispersive X-ray (EDX) unit. Determinations of variations in the Ca^{2+}, and PO_4^{3-} ions were carried out on the collected aliquots by spectrophotometry and atomic absorption spectroscopy (AAS), respectively. Analysis of Ca^{2+} ions concentration was performed

Table 1
Ion concentrations of SBF and 1.5 SBF solutions compared with those of human blood plasma.

	Concentration (mM)							
	Na^+	K^+	Ca^{2+}	Mg^{2+}	HCO_3^-	Cl^-	HPO_4^{2-}	SO_4^{2-}
Blood Plasma	142.0	5.0	2.5	1.5	27.0	103.0	1.0	0.5
SBF	142.0	5.0	2.5	1.0	5.0	131.0	1.0	1.0
1.5 SBF	213.0	7.5	3.75	1.5	7.5	196.5	1.5	1.5

at $\lambda = 442$ nm by AAS using VARIAN-Spectr AA 300 using acetylene with N_2O gases. The KCl releasing buffer with concentration of 4000 ppm was added to each sample. Reproducibility of results was relatively 5–10%. On the other hand, analysis of PO_4^{3-} ions was performed using a SHIMADZU UV-1201 spectrophotometer at a wavelength of 830 nm. Error bars in time dependences represent maximum difference for 2 independent measurements. Changes in the pH of SBF solutions, in which samples were soaked for 2 weeks, were followed by measuring it on the sample surface by a pH-meter.

Phase composition of both neat gypsum and gypsum–polymer composites were also studied by X-ray powder diffraction (XRD) using an automated diffractometer (X'Pert PRO θ–θ), with a step size of 0.02°, counting time of 0.3 s/step and a scan range from 5° to 65° 2θ. A Cu Kα tube operated at 40 kV and 20 mA was used for X-rays generation. XRD patterns were manipulated and interpreted using the ''High Score Plus'' software package.

3. Results and discussion

Compressive strength results of all tested composites compared to polymer-free samples, after curing at ambient conditions for seven days, are shown in Fig. 1. Previous findings showed a progressive increase in the compressive strength of all samples with curing, achieving maximum values after seven days [23]. This was attributed to the completion of hydration of plaster of Paris and its conversion into gypsum as well as the full evaporation of the extra water that was added to improve the workability of the paste. In presence of polymers, all composites showed an overall improvement in their compressive strengths. Comparing composites to each other, the improvement followed the order: Gypsum–PI > Gypsum–PII > Gypsum–PIII. These differences may be explained in terms of the solubility of the original polymers, where PI is totally soluble, PII is slightly soluble, while PIII is insoluble in water. The presence of polymer in solution is thought to facilitate the reaction with the Ca^{2+} ions that are present in the medium during the process of dissolution of plaster and its re-precipitation as gypsum. The formation of calcium salt polymers containing –OH, –COOH, and –COOR groups is known to improve the mechanical properties of composites containing them [25]. On the other hand, the presence of –OH and –COOR groups along the completely insoluble PIII is still thought to be involved in the formation of salts with Ca^{2+} ions in solution through direct reaction with the –OH groups and the hydrolysis of the –COOR groups and the consequent formation of Ca-salts [26]. Due to the insolubility of PIII, the impact of these reactions on the compressive strengths of the obtained composites was not pronounced. Fig. 2 shows SEM micrographs of fractured surfaces of gypsum and its composites after curing for 7 days at ambient conditions. Gypsum is characterized by its high crystallinity and appears as long needles with an average aspect ratio of 7. Strength of polymer-free gypsum samples arises from the mechanical interlocking among the gypsum fibers within the sample, as shown in Fig. 2a. Adding a polymer to these fibers, as shown in Fig. 2b–d, seems to augment them through adsorption on their surfaces. This adsorption, as discussed above, takes place through chemical interaction between each of the polymers and the gypsum fibers. The overall augmented structure, therefore, explains the improvement in the mechanical properties of the composites compared to polymer-free gypsum samples. A closer look at the compressive strength results indicates the progressive enhancement of compressive strength of composites with increasing the polymer in all composites. However, it appears that the presence of excessive amounts of each of the polymers is not recommended as a decrease in the compressive strength values was noticed. Based on these findings, composites containing the optimum concentrations of these polymers were chosen for the preliminary *in vitro* evaluation in protein-free SBF solutions. Those compositions together with a summary of their optimum final setting times and compressive strength values are given in Table 3. An average setting time of 30 ± 2 min was found of all composites.

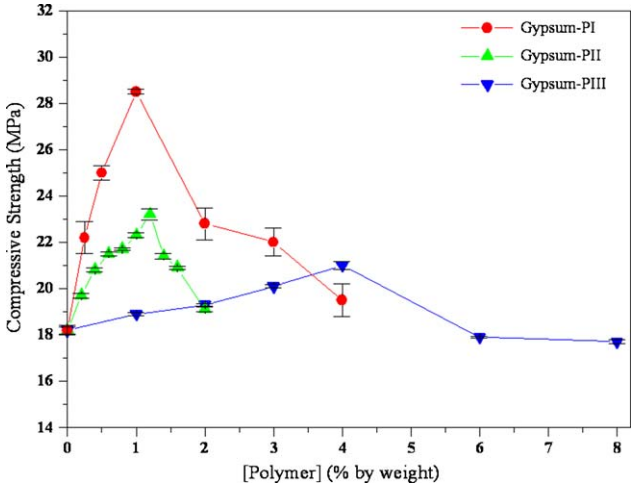

Fig. 1. Compressive strength of gypsum–polymer composites as a function of [polymer] in wt%.

Fig. 3a shows the variations in the concentrations of Ca^{2+} and PO_4^{3-} ions in SBF, as a result of soaking gypsum and its

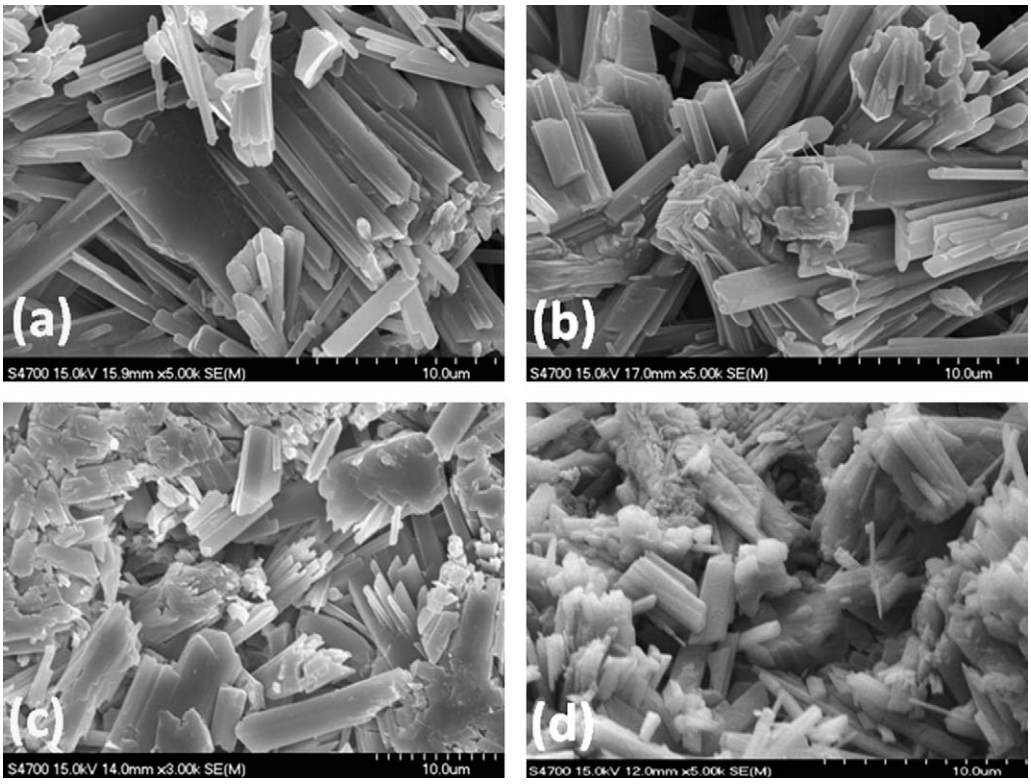

Fig. 2. Scanning electron micrographs of the fractured surfaces of (a) neat gypsum, (b) gypsum–PI, (c) gypsum–PII, and (d) gypsum–PIII composites after curing at ambient conditions for 7 days.

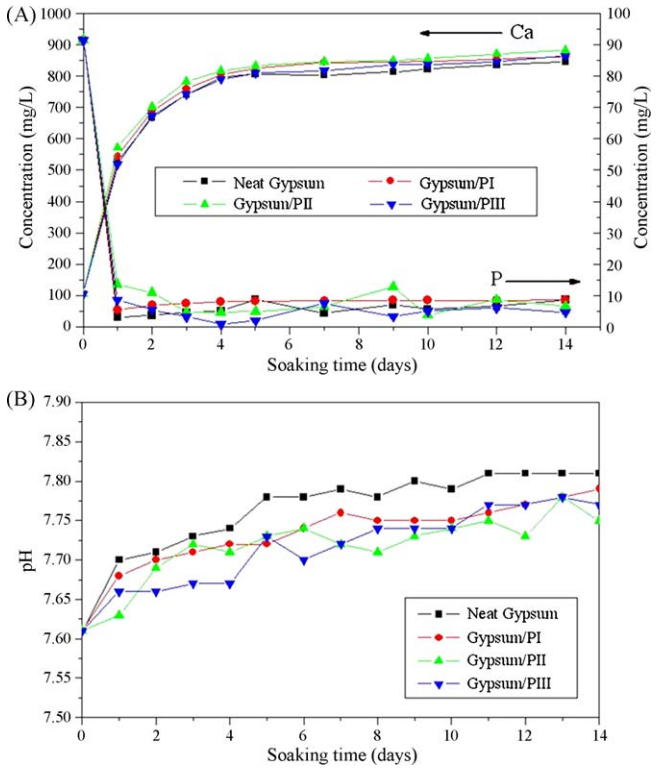

Fig. 3. (a) Total concentrations of Ca and P in SBF solutions after immersing gypsum and gypsum–polymer composites for different time periods. (b) Variations in the pH of SBF solutions as a result of immersing gypsum and gypsum–polymer composites for different time periods.

composites for up to 2 weeks. Concentrations were expressed as total Ca and P in these solutions. A pronounced increase in the concentration of calcium, and a concurrent decrease in the concentration of phosphate, was observed. Deposition of apatite on substrates containing certain functional groups, such as silicates and carboxylates, was previously observed [27]. This process mimics a similar process that takes place in nature, where mineralization of collagen takes place via attracting calcium and phosphate ions from the surrounding body fluids [28–29]. Formation of apatite nuclei is usually followed by growth of these nuclei into apatitic nanocrystals [29]. Mineralization of collagen is attributed to the presence of carboxylic and amino groups along their chains [28]. The currently investigated polymers contain (–COOH) groups along its structures as well as (–OH) and (–COOR) groups. The presence of these groups in the investigated composites are thus considered the sites on which apatite was deposited. Deposition of apatite takes place by consuming Ca^{2+} and PO_4^{3-} ions from solutions, which are known to be supersaturated with respect to apatite. Apatite deposition was thus expected to lead to a decrease in the concentrations of both ions from their solutions

Table 2
Weight loss (%) of gypsum and gypsum–polymer composites after immersion in SBF and 1.5 SBF solutions.

	Gypsum	Gypsum/PI	Gypsum/PII	Gypsum/PIII
SBF	2.9	4.2	4.3	2.4
1.5 SBF	22.9	15.7	15.8	14.3

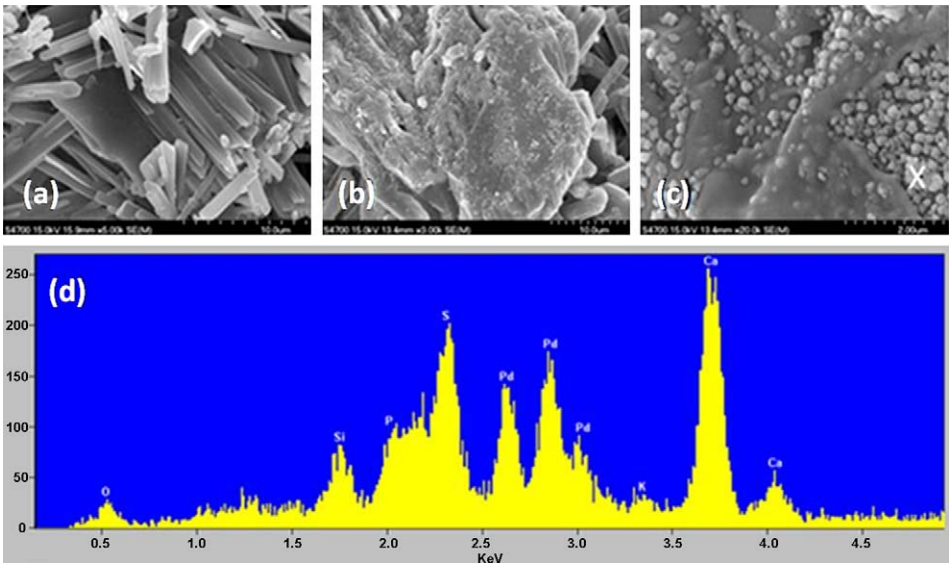

Fig. 4. Scanning electron micrographs of (a) neat gypsum, (b) gyspum after treatment in SBF followed by 1.5 SBF solutions for a week in each, (c) same as in (b) at a higher maginification. (d) Energy-dispersive X-ray analysis of the spot marked by (X) in micrograph (c).

[27]. On the contrary, an increase in the Ca^{2+} concentration in the tested solutions was observed. This is, therefore, attributed to the resorption of gypsum from the investigated composite samples. This trend indicates that the rate of gypsum resorption is higher than the rate of apatite deposition on all surfaces. This was also confirmed by measuring changes in the weight of these samples as a result of the SBF treatment for 2 weeks. Table 2 shows the weight loss observed in all samples, confirming the previous finding that the weight loss due to resorption of gypsum is more pronounced than the weight gain due to deposition of apatite. The rate of resorption, however, is shown to decrease after 4 days, and continued in the same fashion until the end of experiments. These findings were also confirmed by pH measurements where an increase in the solution pH was observed over time, as shown in Fig. 3b. The slow rate of gypsum resorption after 4 days was also reflected in a less pronounced change in the pH of the solutions, achieving a plateau of pH 7.7 $\pm$ 0.05 after 4 days in all samples. Despite the absence of polymers in the neat gypsum samples, similar trends were observed and were confirmed by SEM analysis. Fig. 4a–c shows SEM micrographs of a blank untreated polymer-free gypsum sample as well as polymer-free gypsum samples aged in SBF then 1.5 SBF for a week in each. Fig. 4b shows the formation of a coating on gypsum crystals causing them to agglomerate. Fig. 4c shows a higher magnification of the coating appearing as apatitic spherolites. An elemental analysis of these spherolites was carried out by EDX. The presence of Ca and P in these spherolites is evident, indicating the chemical composition of the coating. The presence of S in the EDX pattern may be attributed to the underlying highly crystalline gypsum crystals. The agglomeration of gypsum crystals as a result of soaking it in SBF and 1.5 SBF solutions may be attributed to the fusion of the gypsum crystals as they undergo degradation. The concurrent precipitation of apatite, therefore, enhanced the gelling of gypsum crystals together. Deposition of apatite on gypsum crystals may be attributed to the increase of [Ca^{2+}] ions in SBF as a result of the resorption of gypsum. As mentioned before, this increase in a solution that is readily supersaturated with respect to apatite should lead to its deposition on the existing surfaces. The SEM/EDX results are thus in accord with those given in Fig. 3a and b for polymer-free gypsum samples. Among the functional groups, that were shown to help in the nucleation of apatite from SBF solutions, is the sulfonate ($-SO_3^-$) group [30]. Previous work by Chan et al. [21] also indicated the formation of apatite from SBF solutions on neat gypsum samples, which is, therefore, in accordance with our current findings, and indicates that sulphate ($-SO_4^-$) groups could also act as nucleating sites for apatite deposition.

Development of phase composition of all samples was followed by X-ray diffraction. Fig. 5 shows XRD patterns of polymer-free gypsum and gypsum composites containing the studied polymers. All patterns showed a complete conversion of plaster of Paris to gypsum, since no peaks of the former phase were detected. Due to the high crystallinity of the gypsum

Table 3
Setting time, and compressive strength values for gypsum and gypsum–polymer composites.

Type of composite	[Polymer] (%)	Setting time (min s)	Compressive strength[a] (MPa)
Neat gypsum	0.0	30 00	18.2 $\pm$ 1.2
Gypsum/PI	1.0	33 15	28.5 $\pm$ 0.1
Gypsum/PII	1.2	33 00	23.2 $\pm$ 0.3
Gypsum/PIII	4.0	27 15	21.0 $\pm$ 0.2

[a] Measurement taken after curing for 7 days at 37 °C.

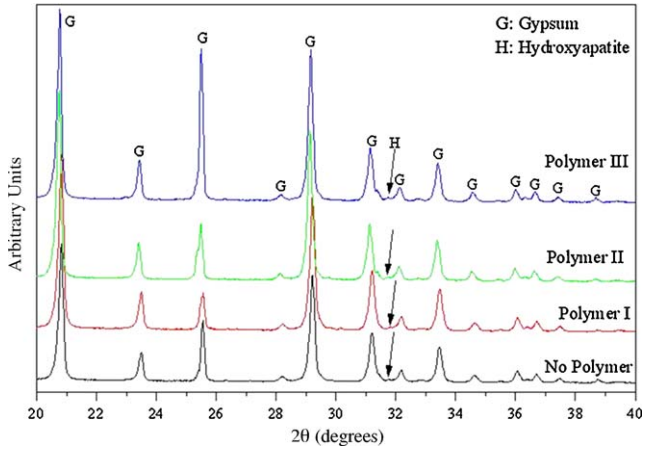

Fig. 5. Phase compositions of gypsum and gypsum–polymer composite solids after immersion I SBF and 1.5 SBF solutions for a week in each.

crystals, its characteristic peaks dominated all patterns, making it difficult to find an evidence for the formation of apatite deposits. However, a closer look at the patterns shows the presence of traces of the 2 1 1 peak of HAp at 2θ value of 31.8°. This peak was found in all samples, with relatively different intensities after treatment in SBF and 1.5 SBF solutions.

The extent of deposition of apatite on polymer-containing composites was variable, depending on the type and structure of the polymer as well as the immersion periods in SBF and 1.5 SBF. Fig. 6a–c shows SEM micrographs of gypsum composites containing the three polymers after 2 weeks of soaking in SBF solutions. The well-known spherolitic morphology of the apatite grown from SBF [31] can be observed in the three Micrographs in Fig. 6a–c and marked by X_1, X_2, and X_3. The elemental composition of these spherolites was also confirmed by EDX analysis, as shown in Fig. 6d for those grown on gypsum–PII composite. It is evident from the micrographs that the extent of apatite deposition was more pronounced in gypsum/PII composites compared to gypsum/PI composites. The presence of –OH groups, as those found along PI chains, are known to bind Ca^{2+} ions from solutions [22]. Therefore, it was expected to see more apatite deposition in gypsum/PI composites than what was actually shown in Fig. 6a. This could be attributed to the high solubility of PI (PVA) in water. The presence of PVA in solution is thought to result in less polymer surfaces that can grow apatite from solution on them. Despite these facts, apatite deposition took place, and was confirmed by EDX. This could be attributed to the deposition of apatite on the PVA thin films immobilized on the formed gypsum crystals, which takes place via bonding to the Ca^{2+} ions in solution that result from the conversion of plaster of Paris into gypsum. On the other hand, the presence of two (–COOH) groups and one (–$COOCH_3$) group in addition to the (–OH) group per monomer of PII rendered the polymer slightly soluble, thus increased the extent of apatite deposition on these active sites. In addition, those groups collectively participated and favoured a higher extent of apatite deposition than composites containing PVA (PI). The presence of apatite deposition on the gypsum composite containing PIII, which is insoluble in water, supports the assumption that both OH and ester groups along the polymer chains participated in the formation of apatite deposits. Additionally, the presence of a highly electronegative atom such as Cl in the polymer structure may also be considered a point of attraction to the positively charged Ca^{2+} ions from solution. Deposition of apatite on the ester (–$COOCH_3$) sites could be related to the local basic hydrolysis of these groups during the conversion of plaster of Paris into gypsum. Similar findings were observed during the treatment of a polyphosphazene, that contains ester groups along its chains, in SBF [26]. Apatite deposition on composites containing PIII, therefore, took place in a slightly different fashion where it

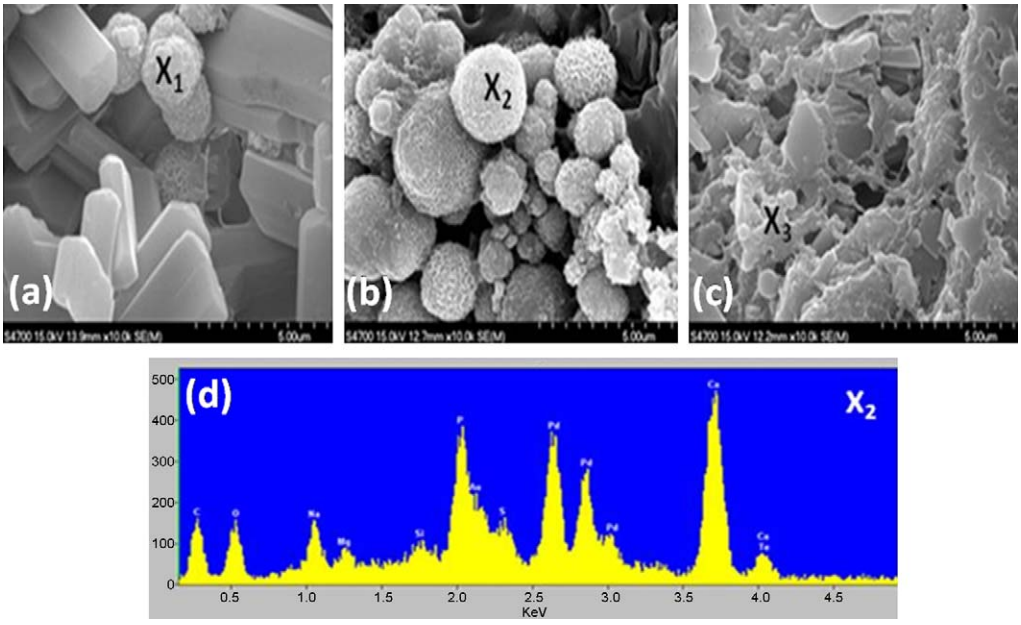

Fig. 6. Scanning electron micrographs of gypsum composites containing (a) polymer I, (b) polymer II, and (c) polymer III after immersion in SBF solutions for 2 weeks, (d) energy-dispersive X-ray analysis of the spot marked by (X) in micrograph (b).

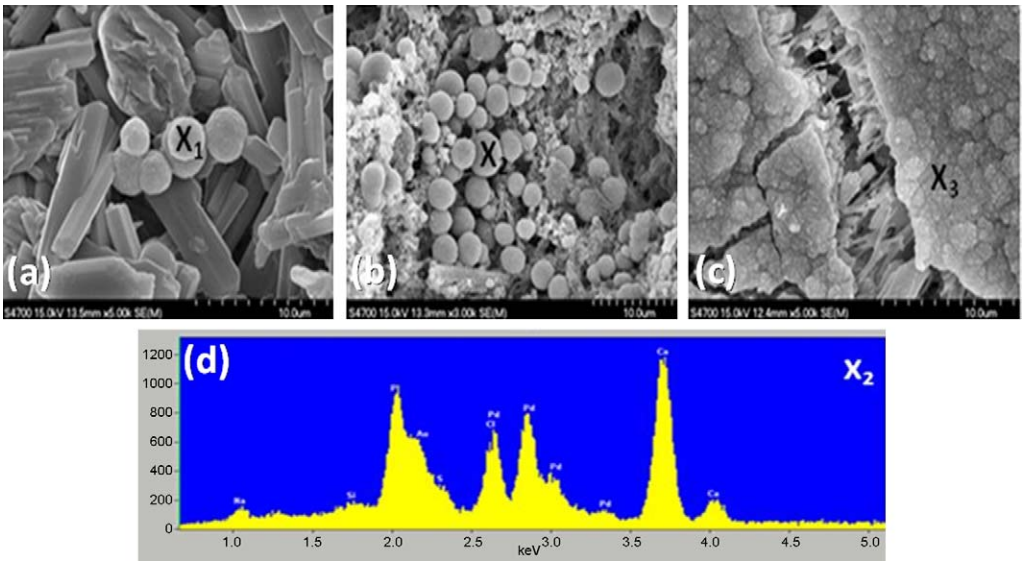

Fig. 7. Scanning electron micrographs of gypsum composites containing (a) polymer I, (b) polymer II, and (c) polymer III after immersion in SBF for 1 week, followed by 1.5 SBF for another week. (d) Energy-dispersive X-ray analysis of the spot marked by (X) in micrograph (b).

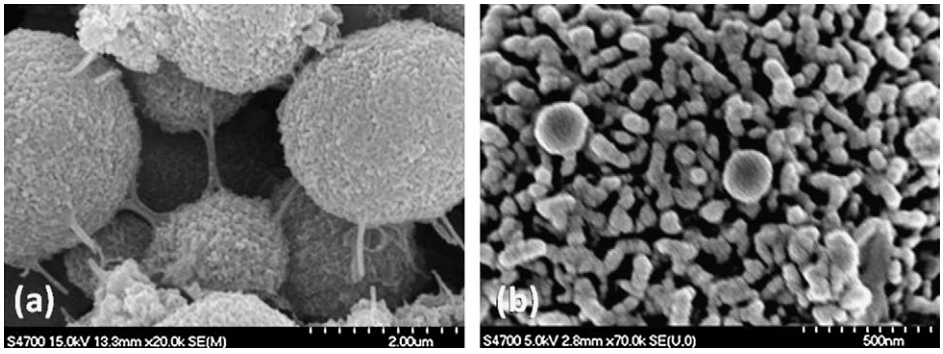

Fig. 8. Scanning electron micrographs of (a) apatite spherolites grown on a gypsum/polymer III composite, and (b) detailed ultrastructure of a spherolite grown on gypsum/polymer III composite.

appeared as continuous layers. Its composition was also confimed by EDX analysis to be apatitic in nature.

Biomimetically deposited apatite spherolites, on solid surfaces, are known to grow if soaked in a highly concentrated SBF solution, in this case called 1.5 SBF [27]. Fig. 7a–c shows SEM micrographs of gypsum–polymer composites after the second treatment in 1.5 SBF solutions for 1 week. Formation of more apatite deposites is evident in all composites compared to those treated in SBF solutions only. Comparing the three composites with each other, the least extent of apatite deposition was found in gypsum–PI composites, while gypsum–PIII composites were found to develop a continuous layer of apatite on their surfaces. Fig. 7d shows an EDX pattern of those spherolites grown on gypsum–PII composites, as an example, confirming the chemical composition of those spherolites to be apatitic in nature. Although apatite deposition on gypsum–PII composites did not take place in the form of layers, the extensive presence of apatite spherolites was reflected in higher intensity Ca and P EDX peaks with lower S peak. Detailed ultrastructure of apatite spherolites grown on gypsum–PIII composites is shown in Fig. 8. The average spherolite size is 2 μm, and each spherolite is made of nanoapatite crystallites with an average dimension of 200 nm. The presence of bridges between the apatite spherolites, shown in Fig. 8a, explains the formation of a continuous apatitic layer on gypsum–PIII composites where apatite spherolites are grown side-by-side on the polymer-coated gypsum crystals.

Taken together, these results clearly indicate the possibility of growing apatite with bone-like morphology on gypsum and its composites, suggesting their potential application as bone cements after being subjected to thorough *in vitro* and *in vivo* evaluations. Moreover, the presence of a bioresorbable gypsum phase in these composites is further expected to result in the formation of pores in a manner that can be synchronized with tissue integration within the set cement after implantation to facilitate the integration of these cements with the surrounding bone tissues after.

4. Summary

Compressive strength was measured for gypsum and its composites with PVA and its copolymers after curing at ambient conditions for 7 days. All Composites showed improved mechanical properties compared to polymer-free

gypsum samples. Composites with highest compressive strengths were further subjected to preliminary *in vitro* evaluation in protein-free SBF solutions. Deposition of apatite spherolites on gypsum–polymer composites was observed with the three different types of polymers used. Moreover, an evidence of the deposition of apatite on polymer-free gypsum samples was also given. Deposition of apatite was concurrent to the normal resorption of gypsum in all samples. Confirmation of the deposition of apatite on all samples was carried out using SEM and EDX techniques. Deposition of apatite on gypsum–polymer composites was attributed to the presence of functional groups along the polymer chains that are known to act as nucleating sites for apatite. Our previous studies showed the formation of chemical bonds between each of the used polymers and gypsum during the process of conversion of plaster of Paris into gypsum. Immobilization of the polymeric chains on gypsum, as a result of their chemical interaction, formed surfaces with nucleating sites for apatite deposition. A water-insoluble copolymer, was, therefore, found to have the greatest extent of apatite coating. On the other hand, the unprecedented deposition of apatite on polymer-free gypsum samples was related to the resorption of gypsum, that resulted in an increase of total [Ca^{2+}] ions in solution exceeding the supersaturating limit of apatite in these solutions. This was consequently followed by precipitation of gel-like apatitic layer on the gypsum crystals, leading to their augmentation, as was observed by the SEM micrographs of these samples and was also supported by their analysis by EDX. Deposition of apatite on the investigated samples indicates their high tendency to bond with bone if used as a bone cement for bone construction. Moreover, the presence of a resorbable fibrous ingredient; gypsum, will provide channels for tissue integration and a consequent enhanced bonding with the surrounding bone. Further *in vitro* and *in vivo* studies are, however, required to fully characterize these composites.

Acknowledgement

This work was a part of the project No 2A-1TP1/063, realized under financial support of the Ministry of industry and trade, Czech Republic. It was also a part of the research programme MSM 6046137302 Preparation and research of functional materials and material technologies using micro- and nanoscopic methods.

References

[1] B. Flautre, J. Lemâitre, C. Maynou, P. Van Landuyt, P. Hardouin, Influence of polymeric additives on the biological properties of brushite cements: an experimental study in rabbit, J. Biomed. Mater. Res. 66A (2003) 214–223.
[2] P. Maragos, N.F. Bissada, R. Wang, R.P. Cole, Comparison of three methods using calcium sulfate as a graft/barrier material for the treatment of class II mandibular molar furcation defects, Int. J. Periodont. Rest. Dent. 22 (2002) 493–501.
[3] C.K. Kim, H.Y. Kim, J.K. Chai, K.S. Cho, I.S. Moon, S.H. Choi, J.S. Sottosanti, U.M. Wikesjo, Periodontal repair in intrabony defects treated with a calcium sulfate implant and calcium sulfate barrier, J. Periodont. 69 (1998) 982–988.
[4] G.E. Pexcora, D. DeLeonardis, C.D. Rocca, R. Cornelini, C. Cortesini, Short-term healing following the use of calcium sulfate as a grafting material for sinus augmentation: a clinical report, Int. J. Oral Max Imp. 13 (1998) 866–873.
[5] M. Nilsson, E. Fernandez, S. Sarda, L. Lidgren, J.A. Planell, Bone-defect healing with calcium-sulfate particles and cement: an experimental study in rabbit, J. Biomed. Mater. Res. 68B (2002) 199–208.
[6] J. Lemâitre, E. Munting, A. Mirtchi, STOMATO 91 (1991) 1–5.
[7] S. Sato, T. Koshino, T. Saito, Osteogenic response of rabbit tibia to hydroxyapatite particle-plaster of paris mixture, Biomaterials 19 (1998) 1895–1900.
[8] P.A. Glazer, U.M. Spencer, R.N. Alkalay, J. Schwardt, In vivo evaluation of calcium sulfate as a bone graft substitute for lumbar spinal fusion, Spine J. 1 (2001) 395–401.
[9] H. Guo, J. Wei, C.S. Liu, Development of a degradable cement of calcium phosphate and calcium sulphate composite for bone reconstruction, Biomed. Mater. 1 (2006) 193–197.
[10] M.A. Rauschmann, T.A. Wichelhaus, V. Stirnal, E. Dingeldein, L. Zichner, R. Schnettler, V. Alt, Nanocrystalline hydroxyapatite and calcium sulphate as biodegradable composite carrier material for local delivery of antibiotics in bone infections, Biomaterials 26 (2005) 2677–2684.
[11] A. Çolak, Characteristics of aqcrylic latex-modified and partially epoxy-impregnated gypsum, Cem. Concr. Res. 31 (2001) 1539–1547.
[12] S. Eve, M. Gomina, J. Hamel, G. Orange, Investigation of the setting of polyamid fiber/latex filled plaster composites, J. Eur. Ceram. Soc. 26 (2006) 2541–2546.
[13] A. Çolak, Physical and mechanical properties of polymer–plaster composites, Mater. Lett. 60 (2006) 1977–1982.
[14] C.K. Chua, K.F. Leong, K.H. Tan, F.E. Wiria, C.M. Cheah, Development of tissue scaffolds using selective laser sintering of polyvinyl alcohol/hydroxyapatite biocomposite for craniofacial and joint defects, J. Mater. Sci. Mater. Med. 15 (2004) 1113–1121.
[15] N. Degirmenbasi, D.M. Kalyon, E. Birinci, Biocomposites of nanohydroxyapatite with collagen and poly(vinyl alcohol), Colloids Surf. B: Biointerfaces 48 (2006) 42–49.
[16] T. Taguchi, A. Kishida, M. Akashi, Apatiteformation on/in hydrogel matrices using an alternate soakingprocess: II. Effect of swelling ratios of poly(vinyl alcohol) hydrogel matrices on apatite formation, J. Biomater. Sci. Polym. Ed. 10 (1999) 331–339.
[17] F.E. Wiria, C.K. Chua, K.F. Leong, Z.Y. Quah, M. Chandrasekaran, M.W. Lee, Improved biocomposite development of poly(vinyl alcohol) and hydroxyapatite for tissue engineering scaffolds fabrication using selective laser sintering, J. Mater. Sci. Mater. Med. 19 (2008) 989–996.
[18] D. Zahn, O. Hochrein, A. Kawska, J. Brickmann, R. Kriep, Towards an atomistic understanding of apatite-collagen biomaterials: linking molecular simulation studies of complex-crystal- and composite-formation to experimental findings, J. Mater. Sci. 42 (2007), 8966-2973.
[19] T. Kokubo, H. Takadama, How useful is SBF in predicting *in vivo* bone bioactivity, Biomaterials 27 (2006) 2907–2915.
[20] M. Bohner, J. Lemaitre, Can bioactivity be tested in vitro with SBF solution? Biomaterials 30 (2009) 2175–2179.
[21] H. Chan, D. Mijares, J.L. Ricci, *In vitro* dissolution of calcium sulphate: evidence of bioactivity, Trans. 7th World Biomater. Congress, 2004, p. 627.
[22] T. Hayami, K. Matsumura, M. Kusunoki, H. Nishikawa, S. Hontsu, Imparting cell adhesion to poly(vinyl alcohol) hydrogel by coating with hydroxyapatite thin film, Mater. Lett. 61 (2007) 2667–2670.
[23] H.F. El-Maghraby, O. Gedeon, A.A. Khalil, Formation and Characterization of Poly(vinyl alcohol-co-vinyl acetate-co-itaconic acid)/Plaster Composites, Part I: Characterization of β-Hemihydrate Plaster, Review of Alexander Dubček University of Trenčin, Slovakia, vol. 1, no. 3, 2007, pp. 39–44, , ISSN 1337-6047.
[24] C. Ohtsuki, T. Kokubo, T. Yamamuro, Mechanism of apatite formation on $CaO–SiO_2–P_2O_5$ glasses in a simulated body fluid, J. Non-cryst. Solids 143 (1992) 84–92.
[25] Y.E. Greish, P.W. Brown, An evaluation of mechanical property and microstructural development in HAp-Ca polycarboxylate biocomposites prepared by hot pressing, J. Biomed. Mater. Res. Appl. Biomater. 53 (2000) 421–429.

[26] Y.E. Greish, J.D. Bender, S. Lakshmi, P.W. Brown, H.R. Allcock, C.T. Laurencin, Low temperature formation of hydroxyapatite-poly(alkyl oxybenzoate)phosphazene composites for biomedical applications, Biomaterials 26 (2005) 1–9.
[27] C. Ohtsuki, H. Kushitani, T. Kokubo, S. Kotani, T. Yamamura, Apatite formation on the surface of ceravital-type glass-ceramic in the body, J. Biomed. Mater. Res. 25 (1991) 1363–1370.
[28] Y.E. Greish, J.D. Bender, S. Lakshmi, P.W. Brown, H.R. Allcock, C.T. Laurencin, Formation of hydroxyapatite-polyphosphazene polymer composites at physiologic temperature, J. Biomed. Mater. Res. 77A (2006) 416–425.
[29] J.F. Shackelford, Bioceramics, Gordon & Breach Science, New York, 1999.
[30] I.B. Leonor, H.–M. Kim, F. Balas, M. Kawashita, R.L. Reis, T. Kokubo, T. Nakamura, J. Mater. Sci. Mater. Med. 18 (2007) 1923–1930.
[31] T. Kokubo, A/W glass-ceramic: processing and properties, in: L.L. Hench, J. Wilson (Eds.), An Introduction to Bioceramics, World Scientific Advanced, Singapore, 1993, pp. 75–88.